HIGH PRECISION SYNCHRONOUS TOOL PATH TRACKING WITH AN AMB MACHINE TOOL SPINDLE

Stephan Eckhardt, Joachim Rudolph
Institut für Regelungs- und Steuerungstheorie, Technische Universität Dresden, Germany
{eckhardt,rudolph}@erss11.et.tu-dresden.de

ABSTRACT

High precision tool path tracking with magnetically supported spindles is considered. It is shown how a new choice of the flat output used may facilitate the control design. Results from simulations and experiments illustrates the usefulness of the approach.

INTRODUCTION

Using active magnetic bearings in machine tool spindles makes it possible to drill non-circular holes. This is achieved by prescribing the path of a single cutting edge on the tool. This motion must be synchronized with the spindle rotation. A high precision synchronous tool path tracking problem results. It can be solved either by moving the whole spindle parallel to its axis of symmetry or by fixing an arbitrary point on this axis. The latter then generates a cone. Of course, such motion is of very restricted amplitude.

There is an industrial demand for such spindles which should allow non-circular motion of the order of 50 micro-meters. The precision required is very demanding, path tracking errors must be less than 1 micro-meter on circular paths and 3 micro-meters on non-circular ones. Typical rotational velocities are up to 10000 rpm. This problem is the subject of a cooperation with Axomat GmbH (see also [4]). Several types of spindles have been constructed and tested.

The control is realized as a cascade, with a current controller in the inner and a position controller in the outer loop. The inner loop can be characterized as a model predictive deadbeat controller which is based on the "electric model" of the bearing coils. The outer loop is based on the rigid body "mechanical model" together with the model for the static relation between the bearing currents, the air gap lengths, and the bearing forces. A nonlinear model is used for that. The control design follows the flatness based control paradigm. Several solutions of this type have been proposed in the literature [1, 4, 3].

Compared to the references cited, in the present contribution a simplification of the approach is proposed which relies on the use of a flat output consisting of the positions of the rotor in two planes perpendicular to the spindle symmetry axis. These planes can be freely chosen. Choosing the plane of motion of the cutting edge as one of them is particularly useful. The other plane is chosen somewhere at the other end of the rotor. Tracking error dynamics for the motion in these planes may then be chosen independently. This can be done using moving frames also, which yields invariance w.r.t. the choice of the coordinates (see [2] for the theory of invariant tracking control). Another advantage is the possibility to achieve high precision tool path tracking while reducing bearing force variations (vibrations, thus). The parameterization of the dynamics is simplified, too.

The paper has the following structure: In the next section a description of the equipment is given, then a mathematical model is introduced. After this, three variants of the flatness based controller design are detailed. They differ in the choice of flat outputs and tracking errors, respectively. Results from simulations and experiments illustrate the usefulness of the approach. High precision tool path tracking is shown to be achieved.

DESCRIPTION OF THE DEVICE

A typical spindle used in our laboratory equipment is the following. The rotor (about 0,6 m long, 10 kg) is levitated by two three-phase electromagnetic radial bearings, arranged like 3 coupled "horseshoe magnets" around the rotor (see Figure 2) and a classical axial disc bearing. The drive is an induction motor. Figure 1 shows a laboratory spindle, industrial ones are of a similar type from the control point of view but have a different housing.

The rotor position and orientation is measured with two pairs of eddy current sensors in two planes perpendicular to the axis of symmetry and another one for the axial rotor position. The angular position for rotation about the longitudinal axis is measured with a contact free incremental sensor. This measurement is needed to synchronize the tool path with the rotation. In the laboratory spindle power amplifiers used are switched transistor bridges the duty ratios of which serve as the eight independent controls (3 per radial bearing, 2 on the axial

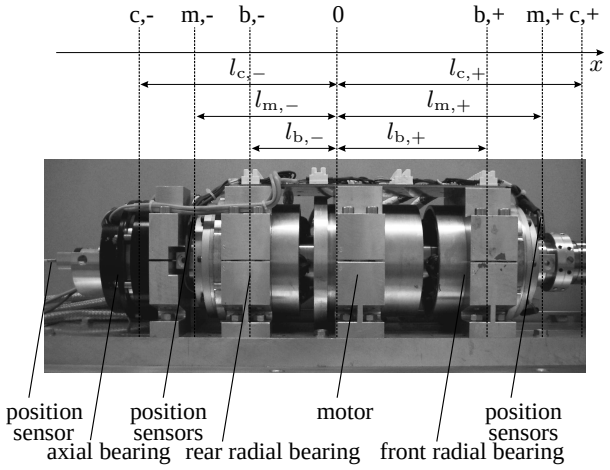

FIGURE 1: Photograph of a laboratory spindle.

one). Designs of current control loops can be tested with these amplifiers. In industrial equipments current controlled amplifiers are used. The computer hardware on the test-bench is a dSpace 1103.

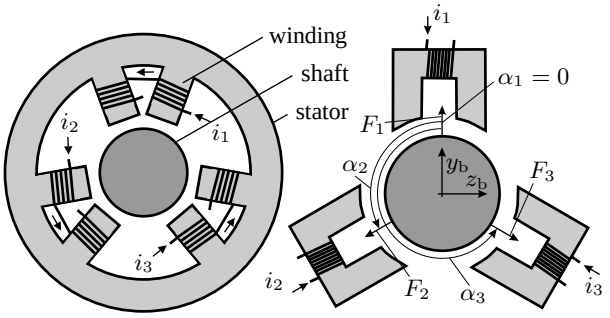

FIGURE 2: Sketch of the three-phase radial bearing and simplified horseshoe type decoupled model.

MATHEMATICAL MODEL

The mathematical model of the spindle is based on the rigid body assumption, and the dynamic equations can be written as follows.

$$
\begin{aligned}
m\,\ddot{X} &= F_{x,+} + F_{x,-} + m\,g_x \\
m\,\ddot{Y} &= F_{y,+} + F_{y,-} + m\,g_y \\
m\,\ddot{Z} &= F_{z,+} + F_{z,-} + m\,g_z \\
J_2\,\ddot{\psi} &= -(l_{\mathrm{b},+} - X)F_{z,+} + (l_{\mathrm{b},-} + X)F_{z,-} - J_1\,\dot{\phi}\,\dot{\theta} \\
J_2\,\ddot{\theta} &= (l_{\mathrm{b},+} - X)F_{y,+} - (l_{\mathrm{b},-} + X)F_{y,-} + J_1\,\dot{\phi}\,\dot{\psi} \\
J_1\,\ddot{\phi} &= D_\phi
\end{aligned}
$$

Here X, Y, and Z are the coordinates of the center of mass of the rotor in a Cartesian frame (with axes x, y, and z) which is fixed in space, at a point being considered as the "center" of the device. The angles ϕ, ψ, and θ describe the angular position of the axes of a body-fixed frame. As the motion is restricted by the small lengths of the air gaps, the Euler angles (Bryant angles) ψ, θ can be interpreted as angles made with the x-axis (the axis of symmetry of the device). The components of the forces, $F_{x,-}$ etc., are indexed by $+$ and $-$ corresponding to the two bearing planes, which are indicated in Figure 1 together with the corresponding distances $l_{\mathrm{b},-}$ and $l_{\mathrm{b},+}$. The remaining parameters are: the mass m of the (symmetric) rotor, its principal moments of inertia J_1 and J_2, and the gravitational acceleration (g_x, g_y, g_z). Finally, D_ϕ denotes the driving torque.

As further simplifications, gyroscopic forces can be neglected, and the axial displacement X being very small against $l_{\mathrm{b},-}$ and $l_{\mathrm{b},+}$ the axial motion can be decoupled from the radial one. The same holds for the rotation about the x-axis. The control of these two mechanical degrees of freedom (corresponding to X and ϕ) is not considered here. With these assumptions the model can be re-written as

$$
\begin{pmatrix} \ddot{Y} \\ \ddot{Z} \\ \ddot{\psi} \\ \ddot{\theta} \end{pmatrix} = M \begin{pmatrix} F_{y,+} \\ F_{z,+} \\ F_{y,-} \\ F_{z,-} \end{pmatrix} + \begin{pmatrix} g_y \\ g_z \\ 0 \\ 0 \end{pmatrix} \tag{1a}
$$

with

$$
M = \begin{pmatrix} \frac{1}{m} & 0 & \frac{1}{m} & 0 \\ 0 & \frac{1}{m} & 0 & \frac{1}{m} \\ 0 & \frac{-l_{\mathrm{b},+}}{J_2} & 0 & \frac{l_{\mathrm{b},-}}{J_2} \\ \frac{l_{\mathrm{b},+}}{J_2} & 0 & \frac{-l_{\mathrm{b},-}}{J_2} & 0 \end{pmatrix} \tag{1b}
$$

In the simplified model used here, the resulting magnetic forces in the two bearing planes are given by the superposition of forces generated by the horseshoe magnets ($j \in \{+,\ -\}$):

$$
\begin{pmatrix} F_{y,j} \\ F_{z,j} \end{pmatrix} = B \begin{pmatrix} F_{1,j} \\ F_{2,j} \\ F_{3,j} \end{pmatrix} \tag{2}
$$

where

$$
B = \begin{pmatrix} \cos\alpha_{1,j} & \cos\alpha_{2,j} & \cos\alpha_{3,j} \\ \sin\alpha_{1,j} & \sin\alpha_{2,j} & \sin\alpha_{3,j} \end{pmatrix}
$$

The angles occurring in the definition of B are introduced in Figure 2 (an index j being added to distinguish between the bearings).

The individual magnetic forces can be modeled as usual ($j \in \{+,\ -\}, k \in \{1,\ 2,\ 3\}$):

$$
F_{k,j} = \lambda_{k,j} \frac{i_{k,j}^2}{\left(s_j - \begin{pmatrix} \cos\alpha_{k,j} \\ \sin\alpha_{k,j} \end{pmatrix}^T \begin{pmatrix} Y_{\mathrm{b},j} \\ Z_{\mathrm{b},j} \end{pmatrix} \right)^2} \tag{3}
$$

where $Y_{\mathrm{b},j}, Z_{\mathrm{b},j}$ are the positions in the bearing planes, s_j the nominal air gap length and $\lambda_{k,j}$ a constant parameter depending on bearing geometry and materials.

The relations between the positions $Y_{\mathrm{b},j}, Z_{\mathrm{b},j}$ and the measured positions follow by inspecting the respective positions of the axis of symmetry in the bearing planes and the measurement planes and the distances between these planes as introduced in Figure 1.

$$\begin{pmatrix} Y_{\mathrm{b},+} \\ Z_{\mathrm{b},+} \\ Y_{\mathrm{b},-} \\ Z_{\mathrm{b},-} \end{pmatrix} = T_{\mathrm{m,b}} \begin{pmatrix} Y_{\mathrm{m},+} \\ Z_{\mathrm{m},+} \\ Y_{\mathrm{m},-} \\ Z_{\mathrm{m},-} \end{pmatrix} \tag{4}$$

with the matrix $T_{\mathrm{m,b}} = T_{\mathrm{m}} + T_{\mathrm{b}}$ defined using

$$T_{\mathrm{m}} = \frac{1}{l_{\mathrm{m},+} + l_{\mathrm{m},-}} \begin{pmatrix} l_{\mathrm{m},-} & 0 & l_{\mathrm{m},+} & 0 \\ 0 & l_{\mathrm{m},-} & 0 & l_{\mathrm{m},+} \\ l_{\mathrm{m},-} & 0 & l_{\mathrm{m},+} & 0 \\ 0 & l_{\mathrm{m},-} & 0 & l_{\mathrm{m},+} \end{pmatrix}$$

and

$$T_{\mathrm{b}} = \begin{pmatrix} l_{\mathrm{b},+} & 0 & -l_{\mathrm{b},+} & 0 \\ 0 & l_{\mathrm{b},+} & 0 & -l_{\mathrm{b},+} \\ l_{\mathrm{b},-} & 0 & -l_{\mathrm{b},-} & 0 \\ 0 & l_{\mathrm{b},-} & 0 & -l_{\mathrm{b},-} \end{pmatrix}$$

CONTROLLER DESIGN

The controller has a cascade structure. The inner controller is used to follow a current reference which is generated by the position controller of the outer loop. The static relation between forces and currents can be used to select force inputs which serve as the controls of a flatness-based position tracking controller. This latter is based on the rigid body model.

In the following, the by now well-known flatness-based design using the rigid body coordinates, i.e., its position and orientation, as components of a flat output (cf. [4, 1]) is discussed. After this a new design is proposed, which is based on coordinates that are more intimately related to the application in mind, namely position coordinates in two so-called control planes (see Figure 1 again). This provides a more direct interpretation of the design, which considerably simplifies the parameterization of the control law.

Two control designs of this type are discussed, one making use of Cartesian error coordinates in frames fixed in either one of the two control planes, the other one using moving frames. Independent error behaviors can be chosen for the motion in the control planes. For this discussion forces are considered as the control inputs.

The method used to calculate the currents is the same for either of the position control approaches. It is, therefore, described after the discussion of the different position control loops.

Position and orientation based errors

In previous work [1, 4, 3] the rigid body position (Y, Z) and angles ψ, θ have been used in the control design. They are related to the measurements, i.e., to the positions of the axis of symmetry of the rotor in two so-called measurement planes (see Figure 1 again), by the following transformation:

$$\begin{pmatrix} Y \\ Z \\ \psi \\ \theta \end{pmatrix} = T_{\mathrm{m},0} \begin{pmatrix} Y_{\mathrm{m},+} \\ Z_{\mathrm{m},+} \\ Y_{\mathrm{m},-} \\ Z_{\mathrm{m},-} \end{pmatrix}$$

where

$$T_{\mathrm{m},0} = \frac{1}{l_{\mathrm{m},+} + l_{\mathrm{m},-}} \begin{pmatrix} l_{\mathrm{m},-} & 0 & l_{\mathrm{m},+} & 0 \\ 0 & l_{\mathrm{m},-} & 0 & l_{\mathrm{m},+} \\ 0 & -1 & 0 & 1 \\ 1 & 0 & -1 & 0 \end{pmatrix}$$

The tracking error may then be defined as

$$e = \begin{pmatrix} e_y \\ e_z \\ e_\psi \\ e_\theta \end{pmatrix} = \begin{pmatrix} Y^{\mathrm{ref}} \\ Z^{\mathrm{ref}} \\ \psi^{\mathrm{ref}} \\ \theta^{\mathrm{ref}} \end{pmatrix} - \begin{pmatrix} Y \\ Z \\ \psi \\ \theta \end{pmatrix} \tag{5}$$

and a simple (yet classical) choice of an error dynamics is the one of 4 decoupled linear oscillators:

$$\ddot{e} + K_1 \dot{e} + K_0 e = 0$$

where K_0 and K_1 are diagonal matrices with real positive entries. Introducing accelerations $a_y, a_z, a_\psi, a_\theta$ as auxiliary variables this can be solved as

$$\begin{pmatrix} a_y \\ a_z \\ a_\psi \\ a_\theta \end{pmatrix} = \begin{pmatrix} \ddot{Y} \\ \ddot{Z} \\ \ddot{\psi} \\ \ddot{\theta} \end{pmatrix} = \begin{pmatrix} \ddot{Y}^{\mathrm{ref}} \\ \ddot{Z}^{\mathrm{ref}} \\ \ddot{\psi}^{\mathrm{ref}} \\ \ddot{\theta}^{\mathrm{ref}} \end{pmatrix} + K_1 \dot{e} + K_0 e$$

Then the corresponding forces are obtained from the rigid body model (1) through

$$\begin{pmatrix} F_{y,+} \\ F_{z,+} \\ F_{y,-} \\ F_{z,-} \end{pmatrix} = M^{-1} \left(\begin{pmatrix} a_y \\ a_z \\ a_\psi \\ a_\theta \end{pmatrix} - \begin{pmatrix} g_y \\ g_z \\ 0 \\ 0 \end{pmatrix} \right) \tag{6}$$

Position errors in control planes

In view of the application under consideration it is more convenient to use the position errors in two so-called control planes (Figure 1). The positions of the axis of symmetry in the two control planes are

$$\begin{pmatrix} Y_{\mathrm{c},+} \\ Z_{\mathrm{c},+} \\ Y_{\mathrm{c},-} \\ Z_{\mathrm{c},-} \end{pmatrix} = T_{\mathrm{m,c}} \begin{pmatrix} Y_{\mathrm{m},+} \\ Z_{\mathrm{m},+} \\ Y_{\mathrm{m},-} \\ Z_{\mathrm{m},-} \end{pmatrix}$$

where $T_{\mathrm{m,c}} = T_{\mathrm{m}} + T_{\mathrm{c}}$ with

$$T_{\mathrm{c}} = \begin{pmatrix} l_{\mathrm{c},+} & 0 & -l_{\mathrm{c},+} & 0 \\ 0 & l_{\mathrm{c},+} & 0 & -l_{\mathrm{c},+} \\ l_{\mathrm{c},-} & 0 & -l_{\mathrm{c},-} & 0 \\ 0 & l_{\mathrm{c},-} & 0 & -l_{\mathrm{c},-} \end{pmatrix}$$

Errors may now be defined as

$$e_{\mathrm{c}} = \begin{pmatrix} e_{\mathrm{c},+,y} \\ e_{\mathrm{c},+,z} \\ e_{\mathrm{c},-,y} \\ e_{\mathrm{c},-,z} \end{pmatrix} = \begin{pmatrix} Y^{\mathrm{ref}}_{\mathrm{c},+} \\ Z^{\mathrm{ref}}_{\mathrm{c},+} \\ Y^{\mathrm{ref}}_{\mathrm{c},-} \\ Z^{\mathrm{ref}}_{\mathrm{c},-} \end{pmatrix} - \begin{pmatrix} Y_{\mathrm{c},+} \\ Z_{\mathrm{c},+} \\ Y_{\mathrm{c},-} \\ Z_{\mathrm{c},-} \end{pmatrix} \tag{7}$$

Interpretation of these errors is more obvious than with angles. The error dynamics may be chosen as above (with positive diagonal gains):

$$\ddot{e}_{\mathrm{c}} + K_{1,\mathrm{c}}\dot{e}_{\mathrm{c}} + K_{0,\mathrm{c}}e_{\mathrm{c}} = 0$$

This defines the controller:

$$\begin{pmatrix} a_{\mathrm{c},+,y} \\ a_{\mathrm{c},+,z} \\ a_{\mathrm{c},-,y} \\ a_{\mathrm{c},-,z} \end{pmatrix} = \begin{pmatrix} \ddot{Y}^{\mathrm{ref}}_{\mathrm{c},+} \\ \ddot{Z}^{\mathrm{ref}}_{\mathrm{c},+} \\ \ddot{Y}^{\mathrm{ref}}_{\mathrm{c},-} \\ \ddot{Z}^{\mathrm{ref}}_{\mathrm{c},-} \end{pmatrix} + K_{1,\mathrm{c}}\dot{e}_{\mathrm{c}} + K_{0,\mathrm{c}}e_{\mathrm{c}}$$

and the forces must satisfy

$$\begin{pmatrix} F_{y,+} \\ F_{z,+} \\ F_{y,-} \\ F_{z,-} \end{pmatrix} = M^{-1} \left(T_{\mathrm{c},0} \begin{pmatrix} a_{\mathrm{c},+,y} \\ a_{\mathrm{c},+,z} \\ a_{\mathrm{c},-,y} \\ a_{\mathrm{c},-,z} \end{pmatrix} - \begin{pmatrix} g_y \\ g_z \\ 0 \\ 0 \end{pmatrix} \right) \tag{8}$$

with

$$T_{\mathrm{c},0} = \frac{1}{l_{\mathrm{c},+} + l_{\mathrm{c},-}} \begin{pmatrix} l_{\mathrm{c},-} & 0 & l_{\mathrm{c},+} & 0 \\ 0 & l_{\mathrm{c},-} & 0 & l_{\mathrm{c},+} \\ 0 & -1 & 0 & 1 \\ 1 & 0 & -1 & 0 \end{pmatrix}$$

Errors in moving frames

Pairs of scalar errors can be introduced by considering projections of e_{c} on the axes of frames the origin of which move on a circular path (as would do a point on the rotor surface if the axis of symmetry were fixed in space). Unit vectors in the directions of these coordinate axes and their derivatives are given by

$$\begin{aligned} \tau &= (\cos\phi, \sin\phi), & \nu &= (\sin\phi, -\cos\phi) \\ \dot{\tau} &= -\dot{\phi}\nu, & \dot{\nu} &= \dot{\phi}\tau \\ \ddot{\tau} &= -\dot{\phi}^2\tau - \ddot{\phi}\nu, & \ddot{\nu} &= -\dot{\phi}^2\nu + \ddot{\phi}\tau \end{aligned}$$

Then new error coordinates are defined by $E_{\mathrm{c}} = Re_{\mathrm{c}}$ with

$$R = \begin{pmatrix} \tau & 0 \\ \nu & 0 \\ 0 & \tau \\ 0 & \nu \end{pmatrix}$$

Once again linear error dynamics may be chosen:

$$\ddot{E}_{\mathrm{c}} + K_{1,\mathrm{c}}\dot{E}_{\mathrm{c}} + K_{0,\mathrm{c}}E_{\mathrm{c}} = 0$$

where

$$\begin{aligned} \dot{E}_{\mathrm{c}} &= \dot{R}e_{\mathrm{c}} + R\dot{e}_{\mathrm{c}} \\ \ddot{E}_{\mathrm{c}} &= \ddot{R}e_{\mathrm{c}} + 2\dot{R}\dot{e}_{\mathrm{c}} + R\ddot{e}_{\mathrm{c}} \end{aligned}$$

This leads to

$$\begin{pmatrix} a_{\mathrm{c},+,y} \\ a_{\mathrm{c},+,z} \\ a_{\mathrm{c},-,y} \\ a_{\mathrm{c},-,z} \end{pmatrix} = \begin{pmatrix} \ddot{Y}^{\mathrm{ref}}_{\mathrm{c},+} \\ \ddot{Z}^{\mathrm{ref}}_{\mathrm{c},+} \\ \ddot{Y}^{\mathrm{ref}}_{\mathrm{c},-} \\ \ddot{Z}^{\mathrm{ref}}_{\mathrm{c},-} \end{pmatrix} + R^{-1} \Big(2\dot{R}\dot{e}_{\mathrm{c}} + \ddot{R}e_{\mathrm{c}} + \cdots K_{1,\mathrm{c}}\dot{E}_{\mathrm{c}} + K_{0,\mathrm{c}}E_{\mathrm{c}} \Big)$$

which can be used in (8) to calculate the control forces.

Calculating control currents

As mentioned above, the current references are obtained from the forces, and this relation is independent of the error definition. In order to simplify the notations, symmetric bearings are assumed, i.e., $\alpha_{1,j} = 0°$, $\alpha_{2,j} = 120°$, $\alpha_{3,j} = 240°$.

In each of the three designs detailed above the result is a pair of independent forces in each of the bearing planes. A third force can be chosen independently. Choosing $F_{1,j}, j \in \{+,-\}$ yields

$$F_{1,j} = \begin{cases} F_{0,j} & \text{if } F_{y,j} \le -\frac{|F_{z,j}|}{\sqrt{3}} \\ F_{0,j} + F_{y,j} + \frac{|F_{z,j}|}{\sqrt{3}} & \text{else} \end{cases}$$

with arbitrary non-negative $F_{0,j}$. The remaining two force components per bearing are obtained from the model (2) of the electro-magnetic part as

$$\begin{aligned} F_{2,j} &= F_{1,j} - F_{y,j} - \frac{F_{z,j}}{\sqrt{3}} \\ F_{3,j} &= F_{1,j} - F_{y,j} + \frac{F_{z,j}}{\sqrt{3}} \end{aligned}$$

Current control inner loops

For the current control loops bearing coils may be considered as independent. Thus, a simplified model comprises an inductance L and a resistance R only. Exact discretization of the linear model

$$\frac{d}{dt}(Li) = u - Ri$$

where L depends on the rotor position, and standard linear discrete time control design is used. The inner loop sampling may be synchronized with the outer loop. Such control is employed on the laboratory test equipment. As an alternative, industrial current controlled amplifiers may be used.

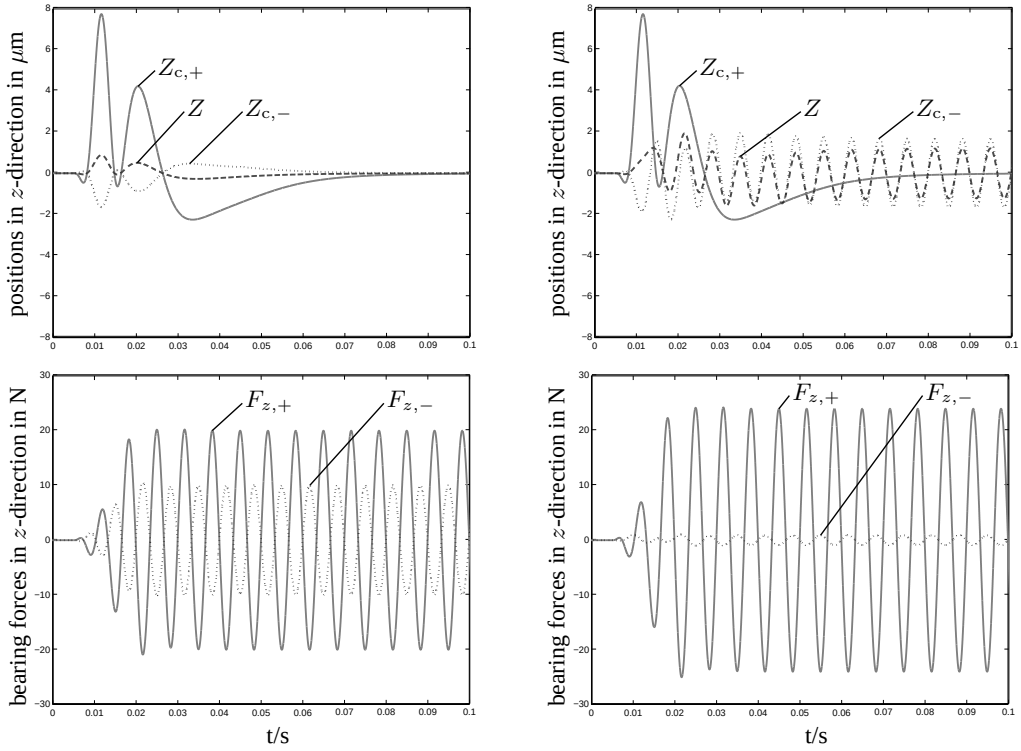

FIGURE 3: Positions and forces in z-direction with position and orientation based errors (left) and position errors in two control planes (right).

Trajectory design and observers

Design of reference trajectories and observers has been discussed at several places, see e.g. [4, 5, 6] and in particular [3].

RESULTS FROM SIMULATIONS AND EXPERIMENTS

In the simulation reported here a rotor turning at 9000 rpm is considered. A force acting in the tool plane is assumed, the amplitude of which increases linearly between $t_0 = 0.015$ s and 0.025 s reaching the final value 20 N, while its direction is synchronous with rotation. This may be considered as simulating a cutting force. The rotor is held at the center position, oriented along the axis of symmetry, i.e., $(Y^{\mathrm{ref}}, Z^{\mathrm{ref}}, \psi^{\mathrm{ref}}, \theta^{\mathrm{ref}}) = (0, 0, 0, 0)$.

First the error defined considering the position of the center of mass and the orientation of the rotor is used. An observer provides estimates of the velocities as well as constant and synchronous harmonic disturbances, as discussed in [4, 5, 6, 3]. Trajectories of the horizontal position and of the bearing forces in z-direction are shown on Figure 3.

Then the position errors in control planes are used (fixed frames). One of the control planes lies in the tool plane, and high precision tracking is achieved in this plane by using the same type of velocity plus disturbance observer as before. The second control plane coincides with the $(\mathrm{b}, -)$-bearing plane and the controller used is designed such as to reduce bearing force variations, which would excite vibrations. Results are given on Figure 3 again.

As can be seen on this figure, with both approaches similar high precision is achieved in the tool plane. However, with the new control design vibrations can be drastically reduced.

In the experiments vibrations result from residual rotor unbalance. (No cutting has been performed here.) These vibrations can be drastically reduced with the new control design, as can be seen on Figure 4. Forces given are calculated from the current references and the measured positions. The tracking error is smaller than 2 μm noise included.

An experimental result of elliptic tool path tracking is given on Figure 5. As above, speed is 9000 rpm, and exact tracking of an elliptic path with 5 and 10 μm axes is required while reducing forces in the $(\mathrm{b}, -)$-bearing.

CONCLUSION

Introducing two control planes and considering the position errors of the rotor axis of symmetry in the control design is an interesting alternative to prior designs. It simplifies the interpretation of the closed-loop behavior, i.e., the choice of controller gains. Furthermore, the

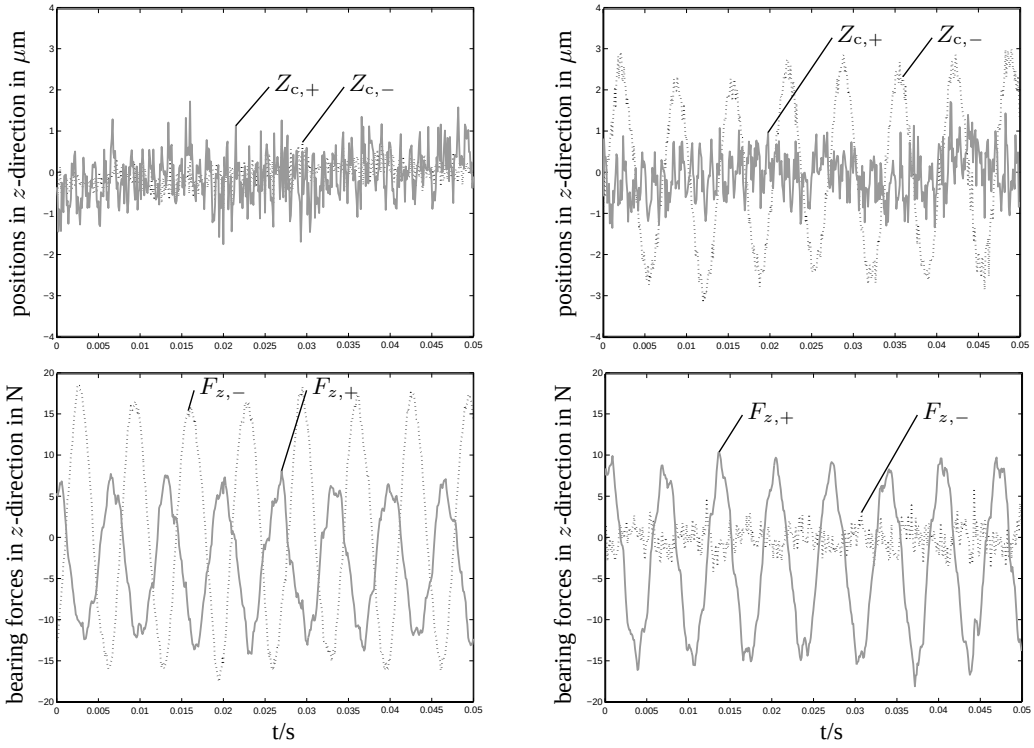

FIGURE 4: Positions and forces in z-direction with position and orientation based errors (left) and position errors in two control planes (right).

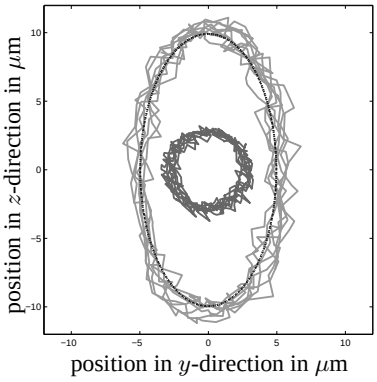

FIGURE 5: Measured paths in the tool plane and the $(\mathrm{b}, -)$-plane (both also used as control planes) with an elliptic reference tool path.

closed-loop can be designed in such a way that high precision tool path tracking is obtained while simultaneously reducing vibrations.

ACKNOWLEDGMENTS

This work has been partially supported by Axomat GmbH, the European Union (EFRE) and the Free State of Saxony (P-No. 5051, 7043) and the Volkswagen Foundation.

REFERENCES

[1] J. Lévine, J. Lottin, and J. C. Ponsart. A nonlinear approach to the control of magnetic bearings. *IEEE Trans. Contr. Syst. Technol.*, 4:524–544, 1996.

[2] Ph. Martin, P. Rouchon, and J. Rudolph. Invariant tracking. *ESAIM: Control, Optimisation and Calculus of Variations*, 3:1–13, 2004.

[3] J. von Löwis. *Flachheitsbasierte Trajektorienfolgeregelung elektromechanischer Systeme*. Berichte aus der Steuerungs- und Regelungstechnik. Shaker Verlag, 2002.

[4] J. von Löwis, J. Rudolph, J. Thiele, and F. Urban. Flatness-based trajectory tracking control of a rotating shaft. In *7th International Symposium on Magnetic Bearings, Zürich*, pages 299–304, 2000.

[5] J. von Löwis, J. Rudolph, and F. Woittennek. Discrete-time flatness-based control of an electromagnetically levitated rotating shaft. In *Proc. 14th Int. Symp. Mathematical Theory of Networks and Systems — mtns 2000*, 2000.

[6] J. von Löwis, J. Rudolph, and F. Woittennek. Zur Regelung einer elektromagnetisch gelagerten Spindel. *at – Automatisierungstechnik*, 48:132–139, 2000.